Electrical Power and Energy Systems 82 (2016) 213–224
Contents lists available at ScienceDirect
Electrical Power and Energy Systems
journal homepage: www.elsevier.com/locate/ijepes

Multi-objective optimal reactive power dispatch using multi-objective differential evolution

M. Basu *

Department of Power Engineering, Jadavpur University, Kolkata 700098, India

ARTICLE INFO

Article history:
Received 5 August 2015
Received in revised form 3 December 2015
Accepted 15 March 2016

Keywords:
Multi-objective optimal reactive power dispatch
Active power transmission loss
Voltage deviation
Voltage stability

ABSTRACT

This paper presents multi-objective differential evolution (MODE) to solve multi-objective optimal reactive power dispatch (MORPD) problem by minimizing active power transmission loss and voltage deviation and maximizing voltage stability while varying control variables such as generator terminal voltages, transformer taps and reactive power output of shunt VAR compensators. MODE has been tested on IEEE 30-bus, 57-bus and 118-bus systems. Numerical results for these three test systems have been compared with those acquired from strength pareto evolutionary algorithm 2 (SPEA 2).

Introduction

Optimal reactive power dispatch (ORPD) perks up power system economy and security. Reactive power generation has no production cost but in general it has an effect on the production cost related with active power transmission loss. Multi-objective optimal reactive power dispatch (MORPD) minimizes active power transmission losses and voltage deviation and maximizes voltage stability simultaneously by adjusting control variables such as generator voltages, transformer tap settings, reactive power output of shunt VAR compensators etc. at the same time satisfying several equality and inequality constraints.

A variety of classical optimization techniques [1–5] such as Newton method, linear programming, quadratic programming and interior point method have been pertained to solve ORPD problem. ORPD is a mixture of discrete and continuous variables with multiple local optima. So it is difficult to acquire global optima by using classical optimization techniques.

In recent times nature-inspired metheuristics such as evolutionary programming (EP) [6], adaptive genetic algorithm (AGA) [7], particle swarm optimization (PSO) [8], hybrid particle swarm optimization (HPSO) [9], bacterial foraging algorithm (BFA) [10], quantum-inspired evolutionary algorithm (QEA) [11], comprehensive learning particle swarm optimization (CLPSO) [12] and hybrid shuffled frog leaping algorithm (HSFLA) and Nelder-Mead simplex search (NMSS) [13] have been pertained to solve ORPD problem.

ORPD problem is formulated as multi-objective optimization problem [14]. The multi-objective problem can be transfer into a single objective problem by weighted sum of objectives [15,16] but it may cause the non-commensurable objectives to lose their importance on merging into a single objective function. Hence, this approach cannot be pertained to find Pareto-optimal solutions of MORPD problems. Classical optimization methods can unearth one solution in one simulation run and therefore these methods are inconvenient to solve multi-objective optimization problems. In case of multi-objective evolutionary algorithms (MOEAs) multiple solutions are unearthed in one simulation run [17].

Recent developed multi-objective evolutionary optimization techniques are non-dominated sorting genetic algorithm (NSGA-II) [22,23], multi-objective differential evolution (MODE) [24], strength pareto evolutionary algorithm (SPEA) [25], pareto archived evolution strategy (PAES) and others. In recent times, SPEA [14,18], NSGA-II [19], hybrid fuzzy multi-objective evolutionary algorithm [20], chaotic parallel vector evaluated interactive honey Bee mating optimization [21] have been pertained to solve multi-objective ORPD (MORPD) problem.

This paper proposes MODE for solving MORPD problem which is formulated by reckoning active power transmission loss minimization, voltage deviation minimization and voltage stability maximization as competing objectives. The proposed technique is validated by applying it to IEEE 30-bus, 57-bus and 118-bus test systems. Test results acquired from the proposed technique are

* Fax: +91 33 23357254.
E-mail address: mousumibasu@yahoo.com

http://dx.doi.org/10.1016/j.ijepes.2016.03.024

compared with those acquired from strength pareto evolutionary algorithm 2 (SPEA 2).

Problem formulation

The MORPD problem is formulated as a true multi-objective optimization problem by reckoning minimization of active power transmission loss and voltage deviation and maximization of voltage stability as objectives at the same time fulfilling equality and inequality constraints. The objective functions and constraints can be stated as:

Objective functions

Minimization of active power transmission loss

The objective function can be stated as:

$$\text{Minimize } F_1 = P_{loss} = \sum_{k=1}^{NTL} g_k[V_i^2 + V_j^2 - 2V_iV_j\cos(\delta_i - \delta_j)] \tag{1}$$

where P_{loss} signifies active power transmission loss, NTL is the number of transmission lines, g_k is the conductance of branch k connected between ith bus and jth bus, V_i and V_j are the magnitude voltage of ith and jth busses, δ_i and δ_j are the phase angle of voltages of the ith and jth busses.

Minimization of voltage deviation

The objective is to minimize the voltage deviation of all load (PQ) busses from 1 p.u to perk up power system security and service quality. The objective function can be stated as:

$$\text{Minimize } F_2 = \sum_{i=1}^{NPQ}|V_i - 1.0| \tag{2}$$

where NPQ is the number of load busses.

Maximization of voltage stability

Voltage stability is the capacity of a power system to keep up suitable voltages at all bus bars beneath normal operating condition and even after disturbances such as change in load demand or system configuration. In recent times a number of major network collapses [28] have been taken place due to voltage instability. Improvement of voltage stability has been acquired by minimizing voltage stability indicator i.e. L – index value at each bus which signifies voltage collapse condition of that bus. L_j of jth bus [29] can be stated as:

$$L_j = \left|1 - \sum_{i=1}^{NPV} F_{ji}\frac{V_i}{V_j}\right| \quad \text{where} \quad j = 1,2,\ldots\ldots,NPQ \tag{3}$$

$$F_{ji} = -[Y_1]^{-1}[Y_2] \tag{4}$$

where NPV is the number of PV bus and NPQ is the number of PQ bus. Y_1 and Y_2 are sub-matrices. YBUS acquired after segregating the PQ and PV bus parameters can be stated as:

$$\begin{bmatrix} I_{PQ} \\ I_{PV} \end{bmatrix} = \begin{bmatrix} Y_1 Y_2 \\ Y_3 Y_4 \end{bmatrix}\begin{bmatrix} V_{PQ} \\ V_{PV} \end{bmatrix} \tag{5}$$

L – index is computed for all PQ busses. L_j is zero or one depending upon no load condition or voltage collapse condition of jth bus. The objective function [27] can be stated as:

$$\text{Minimize} \quad F_3 = \max(L_j), \quad \text{where} \quad j = 1,2,\ldots,NPQ \tag{6}$$

Constraints

Equality constraints

$$P_{Gi} - P_{Di} - V_i\sum_{j=1}^{NB} V_j[G_{ij}\cos(\delta_i - \delta_j) + B_{ij}\sin(\delta_i - \delta_j)] = 0,$$
$$i = 1,2,\ldots,NB \tag{7}$$

$$Q_{Gi} - Q_{Di} - V_i\sum_{j=1}^{NB} V_j[G_{ij}\sin(\delta_i - \delta_j) - B_{ij}\cos(\delta_i - \delta_j)] = 0,$$
$$i = 1,2,\ldots,NB \tag{8}$$

where NB is the number of busses, P_{Gi} and Q_{Gi} are active and reactive power generation at the ith bus, P_{Di} and Q_{Di} are active and reactive power demands at the ith bus, G_{ij} and B_{ij} are the transfer conductance and susceptance between ith bus and jth bus respectively.

Inequality constraints

Generator constraints. The generator voltage magnitudes and reactive power outputs curbed by their minimum and maximum limits can be stated as:

$$V_{Gi}^{min} \leqslant V_{Gi} \leqslant V_{Gi}^{max}, \quad i = 1,2,\ldots,NG \tag{9}$$

$$Q_{Gi}^{min} \leqslant Q_{Gi} \leqslant Q_{Gi}^{max}, \quad i = 1,2,\ldots,NG \tag{10}$$

Shunt VAR compensator constraints. Reactive power output of shunt VAR compensators curbed by their minimum and maximum limits can be stated as:

$$Q_{ci}^{min} \leqslant Q_{ci} \leqslant Q_{ci}^{max}, \quad i = 1,2,\ldots,NC \tag{11}$$

Transformer constraints. Transformer tap settings curbed by their physical deliberation can be stated as:

$$T_i^{min} \leqslant T_i \leqslant T_i^{max}, \quad i = 1,2,\ldots,NT \tag{12}$$

Security constraints. The voltage magnitude of each PQ bus curbed by its minimum and maximum limits and transmission line flow curbed by its maximum limit can be stated as:

$$V_{Li}^{min} \leqslant V_{Li} \leqslant V_{Li}^{max}, \quad i = 1,2,\ldots,NPQ \tag{13}$$

$$S_{li} \leqslant S_{li}^{max}, \quad i = 1,2,\ldots,NTL \tag{14}$$

Principle of multi-objective optimization

Most of the real-world problems involve simultaneous optimization of several objective functions. These functions are non-commensurable and often competing and conflicting objectives. Multi-objective optimization having such conflicting objective functions gives rise to a set of optimal solutions, instead of one optimal solution because no solution can be considered to be better than any other with respect to all objective functions. These optimal solutions are known as pareto-optimal solutions.

Generally, multi-objective optimization problem consisting of a number of objectives and several equality and inequality constraints can be formulated as follows:

$$\text{Minimize} \quad f_i(x) \quad i = 1,\ldots\ldots,N_{obj} \tag{15}$$

$$\text{Subject to} \quad \begin{cases} g_k(x) = 0 & k = 1, \ldots, K \\ h_l(x) \leqslant 0 & l = 1, \ldots, L \end{cases} \tag{16}$$

where f_i is the ith objective function, x is a decision vector.

Multi-objective differential evolution

Differential Evolution (DE) is a type of evolutionary algorithm [26,27] for optimization problems over a continuous domain. DE is exceptionally simple, significantly faster and robust. The basic idea of DE is to adapt the search during the evolutionary process. At the start of the evolution, the perturbations are large since parent populations are far away from each other. As the evolutionary process matures, the population converges to a small region and the perturbations adaptively become small. As a result, DE performs a global exploratory search during the early stages of the evolutionary process and local exploitation during the mature stage of the search. In DE the fittest of an offspring competes one-to-one with that of corresponding parent which is different from other evolutionary algorithms. This one-to-one competition gives rise to faster convergence rate. In multi-objective differential evolution (MODE) [24], a pareto-based approach is introduced to implement the selection of the best individuals.

General approach

Before describing the multi-objective differential evolution (MODE), nondominated sorting procedure, crowded distance estimation procedure and simple crowded comparison operator have been discussed.

Nondominated sorting procedure

In order to identify solutions of the first nondominated front in a population of size N_P, each solution can be compared with every other solution in the population to find if it is dominated. At this stage, all individuals in the first nondominated front are found. In order to find the individuals in the next nondominated front, the solutions of the first front are discounted temporarily and each solution of the remaining population can be compared with every other solution of the remaining population to find if it is dominated. Thus all individuals in the second nondominated front are found. This is true for finding third and higher levels of nondomination.

For each solution two entities are calculated: (a) domination count n_p, the number of solutions which dominate the solution p and (b) S_p, a set of solutions that the solution p dominates. The algorithm for the formation of fast nondominated sort is described below.

Algorithm 1: Non dominated sort

```
for each p ∈ P
  S_p = ϕ
  n_p = 0
  for each q ∈ P
    if (p ≺ q) then   if p dominates q
      S_p = S_p ∪ {q}   add q to the set of solutions dominated
  by p
    else if (q ≺ p) then
      n_p = n_p + 1   increment the domination counter of p
  if n_p = 0 then   p belongs to the first front
    P_rank = 1
  F_1 = F_1 ∪ {p}
```

Each population is assigned a rank equal to its nondomination level or front number (1 is the best level, 2 is the next-best level and so on).

Crowded distance estimation procedure

To get an estimate of the density of solutions surrounding a particular solution in the population, the average distance of two points on either side of this point along each of the objectives is calculated. This quantity serves as an estimate of the perimeter of the cuboid formed by using the nearest neighbors as the vertices. This is called crowding distance. The crowding-distance computation requires sorting the population according to each objective function value in ascending order of magnitude. Thereafter, for each objective function, the boundary populations (populations with smallest and largest function values) are assigned an infinite distance value so that boundary points are always selected. All other intermediate populations are assigned a distance value equal to the absolute normalized difference in the function values of two adjacent populations. This calculation is continued with other objective functions. The overall crowding-distance value is calculated as the sum of individual distance values corresponding to each objective. Each objective function is normalized before calculating the crowding distance.

The algorithm shown below outlines the crowding distance computation procedure of all solutions in an nondominated set F.

Algorithm 2: Crowding distance assignment

```
l = |F|   number of solutions in F
for each i, set F[i]_distance = 0   initialize distance
for each objective m
  F = sort (F, m)   sort using each objective value
  F[1]_distance = F[l]_distance = ∝
  for i = 2 to (l − 1)
    F[i]_distance = F[i]_distance + (F[i + 1] · m − F[i − 1] · m)
                  /(f_m^max − f_m^min)
```

Here, $F[i].m$ refers to the mth objective function value of the ith individual in the set F. f_m^{max} and f_m^{min} are the maximum and minimum values of the mth objective function.

Crowded-comparison operator

The crowded-comparison operator $(\prec)$ guides the selection process at the various stages of the algorithm toward a uniformly spread-out pareto-optimal front. Every individual i in the population has two attributes:

(a) nondomination rank (i_{rank})
(b) crowding distance $(i_{distance})$

$$i \prec j \quad \text{if} \quad i_{rank} < j_{rank} \quad \text{or} \quad ((i_{rank} = j_{rank}) \quad \text{and} \quad (i_{distance} > j_{distance}))$$

Between two populations with differing nondomination ranks, the population with the lower (better) rank is preferred. If both populations belong to the same front, then the population with larger crowding distance is preferred.

Computational flow

Firstly, a population of size, N_P, is generated randomly and objective functions are evaluated. At a given generation of the evolutionary search, the population is sorted into several ranks based on non-domination. Secondly, DE operations are carried out over the individuals of the population. Trial vectors of size N_P are generated and objective functions are evaluated. Both the parent vectors and trial vectors are combined to form a population of size $2N_P$. Then, the ranking of the combined population is carried out followed by the crowding distance calculation. The best N_P individuals are selected based on its ranking and crowding distance. These individuals act as the parent vectors for the next generation. The algorithm of MODE can be described in the following steps:

Step 1. Generate box, R, of size N_P. Parent vectors of size N_P is randomly generated and kept in R.
Step 2. Classify these vectors into fronts based on nondomination [22] as follows:
(a) Create new empty box $R^{/}$ of size N_P.
(b) Compare each vector with all other vectors in R.
(c) Start with $i = 1$.
(d) If ith vector is not dominated by any other vector in R, keep ith vector in $R^{/}$ and go to (f).
(e) If ith vector is dominated by any other vector in R, go to (f).
(f) Increment i by one. If $i \leqslant N_P$, go to (d) otherwise go to (g).
(g) $R^{/}$ now contains a sub-box (of size $\leqslant N_P$) of nondominated vectors, referred to as the first front or sub-box. Assign it a rank number equal to one ($I_{rank} = 1$).
(h) Create subsequent fronts or sub-boxes of $R^{/}$ with the vectors remaining in R and assign these $I_{rank} = 2, 3, \ldots$. Finally, all N_P vectors are in $R^{/}$ into one or more fronts.
Step 3. To calculate the crowding distance, $I_{i,dist}$, for the ith vector in any front, F, of $R^{/}$, sort all the vectors in front, F, according to each objective function value in ascending order of magnitude. The crowding distance of the ith vector in its front F is the average side-length of the cuboid formed by using the nearest neighbors as the vertices. Assign large values of crowding distance I_{dist} to the boundary vectors (vectors with smallest and largest function values).
The following procedure is adopted to identify the better of the two vectors. Vector i is better than vector j (i) if $I_{i,rank} < I_{j,rank}$ or (ii) if $I_{i,rank} = I_{j,rank}$ and $I_{i,dist} > I_{j,dist}$.
Step 4. Take a new empty box $R^{//}$ of size N_P. Perform DE operations over N_P vectors in $R^{/}$ to generate N_P trial vectors and store these vectors in $R^{//}$.
(a) Select a target vector, i in $R^{/}$.
(b) Start with $i = 1$.
(c) Choose two vectors, r_1 and r_2 at random from the N_P vectors in $R^{/}$. Find the vector difference between these two vectors and multiply this difference with the scaling factor F_s to get the weighted difference.
(d) Choose a third random vector r_3 from the N_P vectors in $R^{/}$ and add this vector to the weighted difference to obtain the noisy random vector.
(e) Perform crossover between the target vector and noisy random vector to find the trial vector. This is carried out by generating a random number and if random number $> C_R$ (crossover factor), copy the target vector into the trial vector else copy the noisy random vector into the trial vector and put it in box $R^{//}$.
(f) Increment i by one. If $i \leqslant N_P$, go to (c) otherwise go to Step 5.
Step 5. Copy all N_P parent vectors from $R^{/}$ and all N_P trial vectors from $R^{//}$ into box $R^{///}$. Box $R^{///}$ has $2N_P$ vectors.
(a) Classify these $2N_P$ vectors into fronts based on non-domination and calculate the crowding distance of each vector. Take the best N_P vectors from Box $R^{///}$ and put into Box $R^{////}$.

This completes one generation. Stop if generation number is equal to maximum number of generations. Else copy N_P vectors from Box $R^{////}$ to the starting box R and go to Step 2.

Fig. 1 portrays the flowchart of multi-objective differential evolution.

Best compromise solution

Once the Pareto optimal set is obtained, at the end of the MODE, it is necessary to choose one solution from all non-dominated solutions that represents the best compromise according to the requirements of the decision maker. Due to the imprecise nature of the decision maker's (DM) judgment, it is natural to assume that the DM may have fuzzy or imprecise nature goals of each objective function. Hence, the membership functions are introduced to represents the goals of each objective function; each membership function is defined by the experiences and intuitive knowledge of the decision maker.

In this study, a simple linear membership function portrayed in Fig. 2 and given by Eq. (17) is considered for each of the objective functions.

$$\mu_i = \begin{cases} 0, & \text{if } f_i \geqslant f_i^{\max} \\ \frac{f_i^{\max} - f_i}{f_i^{\max} - f_i^{\min}} & \text{if } f_i^{\min} < f_i < f_i^{\max} \\ 1, & \text{if } f_i \leqslant f_i^{\min} \end{cases} \tag{17}$$

where $f_i^{\min}$ and $f_i^{\max}$ are the minimum and the maximum value of the ith objective function among all non-dominated solutions, respectively. The membership function μ_i is varied between 0 and 1, where $\mu_i = 0$ indicates the incompatibility of the solution with the set, while $\mu_i = 1$ means full compatibility.

For each non-dominated solution k, the normalized membership function μ^k is calculated as follows:

$$\mu^k = \frac{\sum_{i=1}^{N_{obj}} \mu_i^k}{\sum_{k=1}^{M_{nd}} \sum_{i=1}^{N_{obj}} \mu_i^k} \tag{18}$$

where M_{nd} is the number of non-dominated solutions and N_{obj} is the number of objective functions. The function μ_k can be considered as a membership function of non-dominated solutions in a fuzzy set, where the solution having the maximum membership in the fuzzy set is considered as the best compromise solution.

Simulation results

The proposed technique has been pertained to solve MORPD problem and IEEE 30-bus, IEEE 57-bus and IEEE 118-bus systems have been tested to confirm its efficacy. In order to show the efficacy of the proposed MODE technique, SPEA 2 has been pertained to solve the problem. All the algorithms i.e. MODE, SPEA 2 and differential evolution (DE), used in this paper for solving MORPD problem have been executed in MATLAB 7.0 on a PC (Pentium-IV, 80 GB, 3.0 GHz).

In order to explore the extreme points of the trade-off surface, active power transmission loss, voltage deviation and L-index objectives are minimized individually by using DE for all the three test systems.

MODE has been pertained to minimize active power transmission loss, voltage deviation and L-index objectives simultaneously for all the three test systems. For comparison, SPEA 2 has been applied to solve the MORPD problem.

In case of DE, the scaling factor (S_F), crossover rate (C_R) and the maximum iteration number ($N_{\max}$) have been chosen as 1, 0.9 and 100 respectively for all the cases of three test system. The population size is 100 for IEEE 30-bus system and IEEE 57-bus system but for IEEE 118-bus system population size is 200.

In case of MODE and SPEA 2, the population size, maximum number of iterations, scaling factor (S_F) and crossover rate (C_R) have been chosen as 10, 30, 1 and 0.9, respectively for all the three test systems.

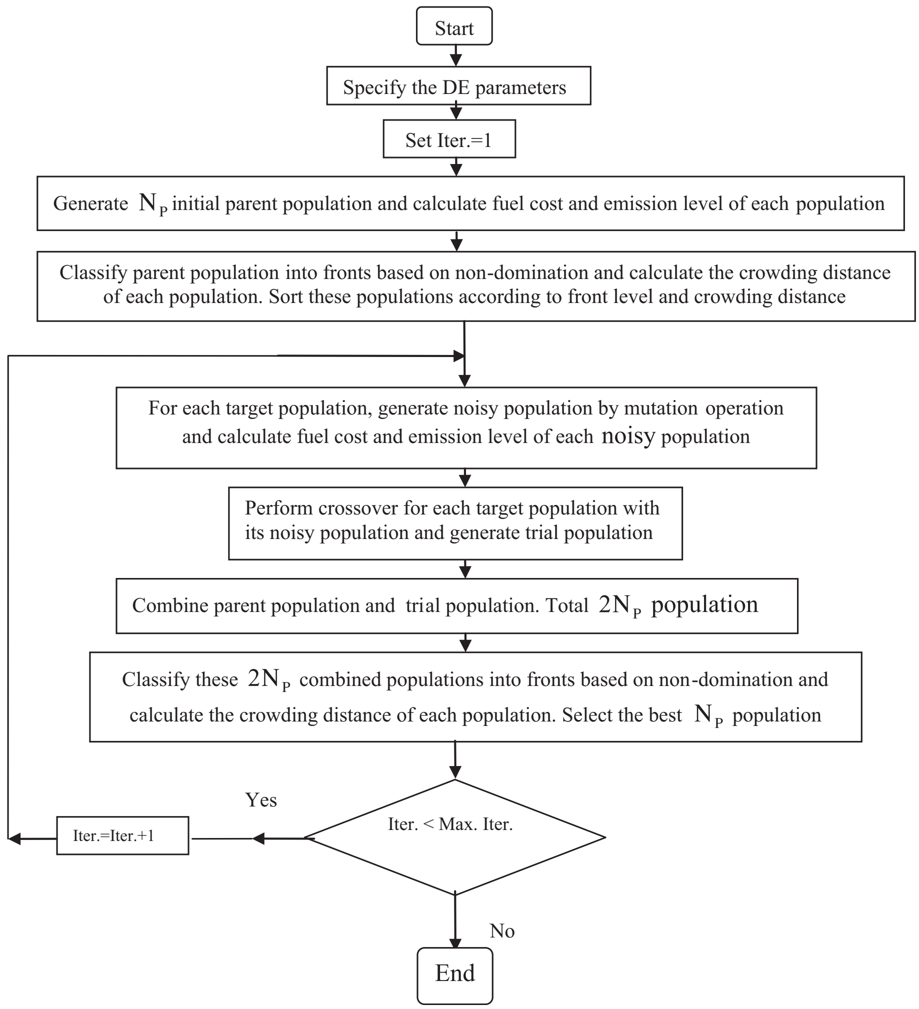

Fig. 1. Flowchart of multi-objective differential evolution.

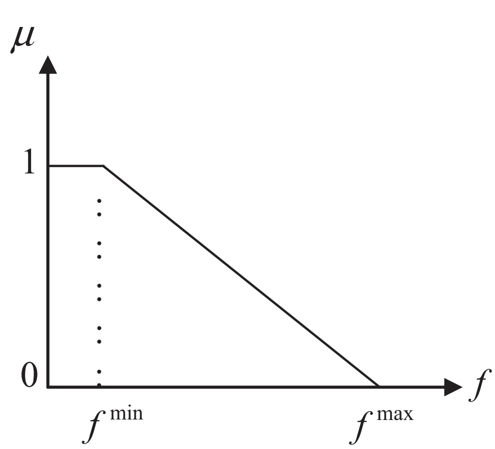

Fig. 2. Linear membership function.

50 runs are carried out for each case for each test system and the best results acquired from 50 runs are given here.

IEEE 30-bus system

The line data, bus data, generator data and the minimum and maximum limits for the control variables have been adapted from [3]. The system has six generators at busses 1, 2, 5, 8, 11 and 13 and four transformers with off nominal tap ratio at lines 6–9, 6–10, 4–12, and 28–27 and shunt VAR compensators are connected at bus bars 10, 12, 15, 17, 20, 21, 23, 24 and 29. Total real power demand is 2.834 p.u. at 100 MVA base.

The optimal control variables and active power transmission loss, voltage deviation, L-index and CPU time acquired from the minimization of active power transmission loss, voltage deviation and L-index by using DE have been summed up in Table 1. The optimal control variables and active power transmission loss, voltage deviation, L-index and CPU time acquired from the best compromise solution of last iteration from proposed from MODE and SPEA 2 have been also summed up in Table 1. The convergence characteristics acquired from active power transmission loss, voltage deviation, L-index minimization by using DE have been portrayed in Fig. 3. The distribution of 10 nondominated solutions acquired from the last iteration of proposed MODE and SPEA 2 for this test system is portrayed in Fig. 4. Fig. 4 portrays the relationship of active power transmission loss, voltage deviation and L-index of nondominated solutions.

IEEE 57-bus system

The standard IEEE 57-bus system consists of 80 transmission lines, seven generators at busses 1, 2, 3, 6, 8, 9, 12 and 15 branches under load tap setting transformer branches. The reactive power

Table 1
Optimal value of control variables acquired from IEEE 30 bus system for different cases.

Control variable	Active power loss minimization	Voltage stability enhancement	Improvement of voltage profile	MORPD MODE	MORPD SPEA 2
V_1	1.0500	1.0500	1.0500	1.0500	1.0500
V_2	1.0338	1.0336	1.0340	1.0338	1.0188
V_5	1.0058	1.0055	1.0059	1.0058	1.0189
V_8	1.0230	1.0232	1.0235	1.0230	1.0197
V_{11}	1.0913	1.0911	1.0917	1.0913	1.0206
V_{13}	1.0400	1.0402	1.0396	1.0400	1.0211
T_{6-9}	0.9994	0.9875	1.0157	0.9979	1.0153
T_{6-10}	1.0012	1.0031	1.0274	1.0035	0.9633
T_{4-12}	0.9983	1.0222	1.0087	1.0007	1.0132
T_{28-27}	1.0141	0.9895	0.9817	1.0049	0.9575
Q_{c10}	0.0030	0.0000	0.0095	0.0000	0.0029
Q_{c12}	0.0199	0.0032	0.0068	0.0095	0.0000
Q_{c15}	0.0475	0.0500	0.0301	0.0500	0.0500
Q_{c17}	0.0334	0.0314	0.0079	0.0620	0.0333
Q_{c20}	0.0182	0.0500	0.0247	0.0451	0.0444
Q_{c21}	0.0250	0.0249	0.0171	0.0256	0.0500
Q_{c23}	0.0342	0.0486	0.0301	0.0128	0.0220
Q_{c24}	0.0345	0.0403	0.0500	0.0500	0.0000
Q_{c29}	0.0000	0.0500	0.0178	0.0409	0.0500
power loss (MW)	2.6867	7.0812	9.2745	4.6801	7.0800
voltage deviation	0.4609	0.8886	0.0607	0.6572	0.6593
L_{max}	0.0581	0.0238	0.0543	0.0507	0.0517
CPU time (sec)	27.78	27.97	28.04	25.56	34.63

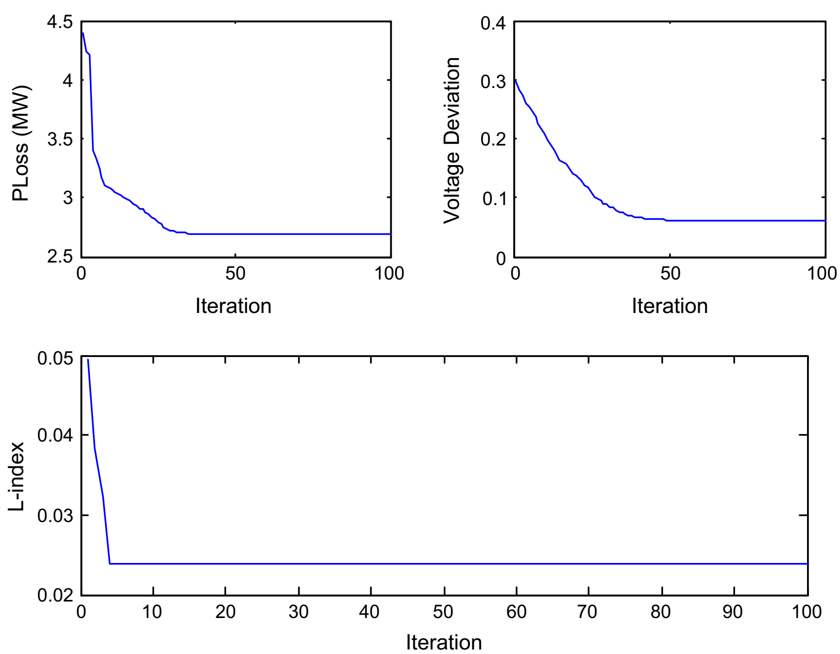

Fig. 3. Active power loss, voltage deviation and L-index convergence characteristics of IEEE 30 bus system.

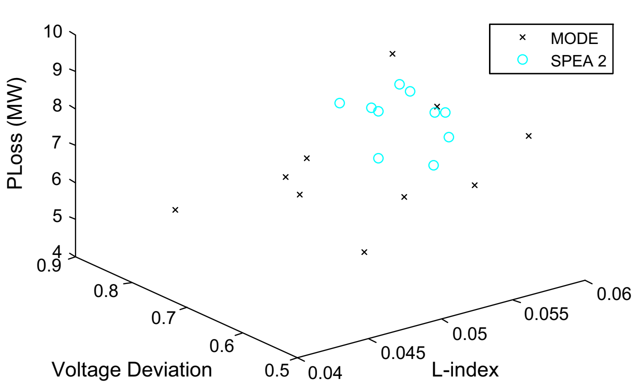

Fig. 4. Pareto-optimal front acquired from the last iteration for IEEE 30 bus system.

sources are considered at busses 18, 25 and 53. The system line data, bus data, generator data and the minimum and maximum limits for the control variables, the upper and lower limits of reactive power sources and transformer tap settings have been adapted from [30]. The total system active power demand is 12.508 p.u. and reactive power demand is 3.364 p.u. at 100 MVA base.

The optimal control variables and active power transmission loss, voltage deviation, L-index and CPU time acquired from the minimization of active power transmission loss, voltage deviation and L-index by using DE have been summed up in Table 2. The optimal control variables and active power transmission loss, voltage deviation, L-index and CPU time acquired from the best compromise solution of last iteration from proposed from MODE and SPEA 2 have been also summed up in Table 2. The convergence

Table 2
Optimal value of control variables acquired from IEEE 57 bus system for different cases.

Control variable	Active power loss minimization	Voltage stability enhancement	Improvement of voltage profile	MORPD MODE	MORPD SPEA 2
V_1	1.0400	1.0400	1.0400	1.0400	1.0400
V_2	1.0101	1.0103	1.0099	1.0100	1.0101
V_3	0.9849	0.9847	0.9851	0.9850	0.9853
V_6	0.9805	0.9800	0.9803	0.9800	0.9804
V_8	1.0054	1.0050	1.0051	1.0050	1.0048
V_9	0.9803	0.9805	0.9804	0.9800	0.9801
V_{12}	1.0147	1.0150	1.0152	1.0150	1.0155
T_{4-18}	1.0987	0.9801	0.9831	0.9805	0.9700
T_{4-18}	1.0820	0.9526	0.9510	0.9529	0.9780
T_{21-20}	0.9221	0.9501	0.9507	0.9505	0.9604
T_{24-26}	1.0171	1.0045	1.0043	1.0047	1.0430
T_{7-29}	0.9960	0.9777	0.9769	0.9775	0.9670
T_{34-32}	1.0999	0.9138	0.9139	0.9136	1.0430
T_{11-41}	1.0750	0.9465	0.9461	0.9463	1.0351
T_{15-45}	0.9541	0.9269	0.9258	0.9265	0.9487
T_{14-46}	0.9370	0.9962	0.9957	0.9960	0.9789
T_{10-51}	1.0160	1.0385	1.0379	1.0388	1.0351
T_{13-49}	1.0998	0.9052	0.9053	0.9048	0.9352
T_{11-43}	1.0980	0.9240	0.9229	0.9245	0.9233
T_{40-56}	0.9799	0.9875	0.9868	0.9877	0.9867
T_{39-57}	1.0246	1.0098	1.0095	1.0092	1.0104
T_{9-55}	1.0371	0.9373	0.9367	0.9375	0.9404
Q_{c18}	0.0488	0.0401	0.0000	0.0405	0.0554
Q_{c25}	0.0012	0.0590	0.0008	0.0433	0.0591
Q_{c53}	0.0001	0.0166	0.0583	0.0174	0.0000
Power loss (MW)	15.8473	34.9690	29.9137	18.8903	20.7699
Voltage deviation	3.6588	1.0947	0.6634	1.1004	1.0920
L_{max}	0.1625	0.0977	2.7554	0.1755	0.1574
CPU time (sec)	49.53	49.67	49.93	47.77	61.79

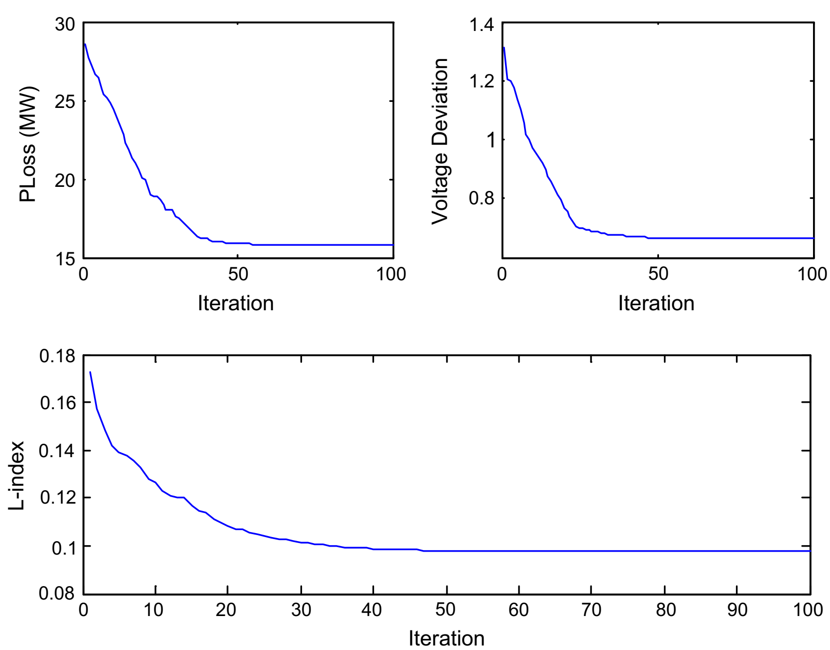

Fig. 5. Active power loss, voltage deviation and L-index convergence characteristics of IEEE 57 bus system.

characteristics acquired from active power transmission loss, voltage deviation, L-index minimization by using DE have been portrayed in Fig. 5. The distribution of 10 nondominated solutions acquired from the last iteration of proposed MODE and SPEA 2 for this test system is portrayed in Fig. 6. Fig. 6 portrays the relationship of active power transmission loss, voltage deviation and L-index of nondominated solutions.

IEEE 118-bus system

The standard IEEE 118-bus system consists of 186 transmission lines, 54 generator busses, 64 load busses, 9 branches under load tap setting transformer and 14 reactive power sources. The system line data, bus data, generator data and the minimum and maximum limits for the control variables, the upper and lower limits of reactive power sources and transformer tap settings have been

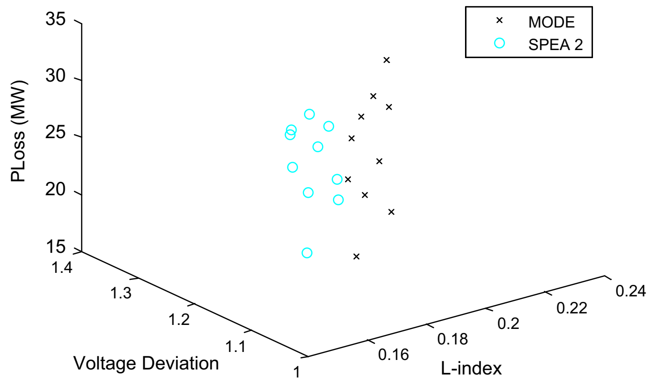

Fig. 6. Pareto-optimal front acquired from the last iteration for IEEE 57 bus system.

Table 3
Optimal value of control variables acquired from active power loss minimization for IEEE 118 bus system.

Variable	
V_1	0.9552
V_4	0.9984
V_6	0.9907
V_8	1.0151
V_{10}	1.0500
V_{12}	0.9903
V_{15}	0.9701
V_{18}	0.9730
V_{19}	0.9654
V_{24}	0.9920
V_{25}	1.0500
V_{26}	1.0154
V_{27}	0.9680
V_{31}	0.9671
V_{32}	0.9682
V_{34}	0.9853
V_{36}	0.9793
V_{40}	0.9700
V_{42}	0.9850
V_{46}	1.0050
V_{49}	1.0250
V_{54}	0.9550
V_{55}	0.9516
V_{56}	0.9543
V_{59}	0.9850
V_{61}	0.9950
V_{62}	0.9980
V_{65}	1.0050
V_{66}	1.0500
V_{69}	1.0350
V_{70}	0.9857
V_{72}	0.9800
V_{73}	0.9910
V_{74}	0.9655
V_{76}	0.9422
V_{77}	1.0058
V_{80}	1.0400
V_{85}	0.9885
V_{87}	1.0150
V_{89}	1.0050
V_{90}	0.9800
V_{91}	0.9835
V_{92}	0.9724
V_{99}	1.0103
V_{100}	0.9693
V_{103}	0.9532
V_{104}	0.9370
V_{105}	0.9396
V_{107}	0.9520
V_{110}	0.9567
V_{111}	0.9800
V_{112}	0.9750
V_{113}	0.9930
V_{116}	1.0050
T_{8-5}	0.9811
T_{26-25}	0.9603
T_{30-17}	0.9611
T_{38-37}	0.9360
T_{63-59}	0.9598
T_{64-61}	0.9847
T_{65-66}	0.9349
T_{68-69}	0.9345
T_{81-82}	0.9359
Q_{c5}	−0.2599
Q_{c34}	0.0218
Q_{c37}	−0.0145
Q_{c44}	0.0678
Q_{c45}	0.0644
Q_{c46}	0.0000
Q_{c48}	0.0992
Q_{c74}	0.0771
Q_{c79}	0.0852
Q_{c82}	0.1203
Q_{c83}	0.0805
Q_{c105}	0.0828
Q_{c107}	0.1975
Q_{c110}	0.0005
Power loss (MW)	80.9257
Voltage deviation	2.0904
L_{max}	0.1100
CPU time (s)	80.07

Table 4
Optimal value of control variables acquired from L-index minimization for IEEE 118 bus system.

Variable	
V_1	0.9548
V_4	0.9975
V_6	0.9901
V_8	1.0153
V_{10}	1.0500
V_{12}	0.9901
V_{15}	0.9703
V_{18}	0.9729
V_{19}	0.9652
V_{24}	0.9924
V_{25}	1.0497
V_{26}	1.0153
V_{27}	0.9685
V_{31}	0.9671
V_{32}	0.9695
V_{34}	0.9838
V_{36}	0.9800
V_{40}	0.9705
V_{42}	0.9851
V_{46}	1.0053
V_{49}	1.0253
V_{54}	0.9550
V_{55}	0.9529
V_{56}	0.9556
V_{59}	0.9851
V_{61}	0.9953
V_{62}	0.9984
V_{65}	1.0052
V_{66}	1.0504
V_{69}	1.0350
V_{70}	0.9868
V_{72}	0.9807
V_{73}	0.9911
V_{74}	0.9623
V_{76}	0.9430
V_{77}	1.0061
V_{80}	1.0404
V_{85}	0.9888

Table 4 (*continued*)

Variable	
V_{87}	1.0153
V_{89}	1.0055
V_{90}	0.9853
V_{91}	0.9800
V_{92}	1.0039
V_{99}	1.0101
V_{100}	1.0172
V_{103}	1.0039
V_{104}	0.9756
V_{105}	0.9702
V_{107}	0.9520
V_{110}	0.9730
V_{111}	0.9803
V_{112}	0.9751
V_{113}	0.9933
V_{116}	1.0051
T_{8-5}	0.9805
T_{26-25}	0.9602
T_{30-17}	0.9607
T_{38-37}	0.9351
T_{63-59}	0.9597
T_{64-61}	0.9848
T_{65-66}	0.9345
T_{68-69}	0.9346
T_{81-82}	0.9353
Q_{c5}	−0.3278
Q_{c34}	0.0000
Q_{c37}	−0.1635
Q_{c44}	0.0521
Q_{c45}	0.0905
Q_{c46}	−0.3338
Q_{c48}	0.0324
Q_{c74}	0.0000
Q_{c79}	0.1860
Q_{c82}	0.1253
Q_{c83}	0.1362
Q_{c105}	0.0000
Q_{c107}	−0.1278
Q_{c110}	0.0693
Power loss (MW)	114.45
Voltage deviation	1.6884
L_{max}	0.0619
CPU time (s)	80.35

Table 5
Optimal value of control variables acquired from voltage deviation minimization for IEEE 118 bus system.

Variable	
V_1	0.9553
V_4	0.9981
V_6	0.9905
V_8	1.0152
V_{10}	1.0498
V_{12}	0.9901
V_{15}	0.9706
V_{18}	0.9731
V_{19}	0.9655
V_{24}	0.9923
V_{25}	1.0500
V_{26}	1.0151
V_{27}	0.9683
V_{31}	0.9672
V_{32}	0.9711
V_{34}	0.9846
V_{36}	0.9820
V_{40}	0.9703
V_{42}	0.9851
V_{46}	1.0054
V_{49}	1.0253
V_{54}	0.9551
V_{55}	0.9557
V_{56}	0.9565

Table 5 (*continued*)

Variable	
V_{59}	0.9849
V_{61}	0.9953
V_{62}	0.9981
V_{65}	1.0054
V_{66}	1.0500
V_{69}	1.0350
V_{70}	0.9871
V_{72}	0.9803
V_{73}	0.9908
V_{74}	0.9634
V_{76}	0.9431
V_{77}	1.0063
V_{80}	1.0401
V_{85}	0.9891
V_{87}	1.0153
V_{89}	1.0051
V_{90}	0.9853
V_{91}	0.9804
V_{92}	0.9994
V_{99}	1.0100
V_{100}	1.0171
V_{103}	1.0044
V_{104}	0.9768
V_{105}	0.9737
V_{107}	0.9520
V_{110}	0.9733
V_{111}	0.9801
V_{112}	0.9754
V_{113}	0.9929
V_{116}	1.0051
T_{8-5}	0.9848
T_{26-25}	0.9601
T_{30-17}	0.9603
T_{38-37}	0.9351
T_{63-59}	0.9605
T_{64-61}	0.9849
T_{65-66}	0.9347
T_{68-69}	0.9351
T_{81-82}	0.9354
Q_{c5}	−0.3398
Q_{c34}	−0.1214
Q_{c37}	−0.1308
Q_{c44}	0.0835
Q_{c45}	0.0973
Q_{c46}	0.0000
Q_{c48}	0.0649
Q_{c74}	0.0000
Q_{c79}	0.0824
Q_{c82}	0.1579
Q_{c83}	0.0123
Q_{c105}	0.0000
Q_{c107}	0.0000
Q_{c110}	0.0316
Power loss (MW)	83.9356
Voltage deviation	1.6008
L_{max}	0.0674
CPU time (s)	80.97

Table 6
Optimal value of control variables acquired from MODE for IEEE 118 bus system.

Variable	
V_1	0.9556
V_4	0.9979
V_6	0.9904
V_8	1.0150
V_{10}	1.0477
V_{12}	0.9903
V_{15}	0.9715
V_{18}	0.9732
V_{19}	0.9649
V_{24}	0.9921
V_{25}	1.0500

(*continued on next page*)

Table 6 (*continued*)

Variable	
V_{26}	1.0153
V_{27}	0.9684
V_{31}	0.9672
V_{32}	0.9689
V_{34}	0.9835
V_{36}	0.9803
V_{40}	0.9709
V_{42}	0.9856
V_{46}	1.0055
V_{49}	1.0252
V_{54}	0.9556
V_{55}	0.9563
V_{56}	0.9569
V_{59}	0.9848
V_{61}	0.9955
V_{62}	0.9986
V_{65}	1.0051
V_{66}	1.0500
V_{69}	1.0350
V_{70}	0.9875
V_{72}	0.9806
V_{73}	0.9911
V_{74}	0.9632
V_{76}	0.9434
V_{77}	1.0062
V_{80}	1.0415
V_{85}	0.9867
V_{87}	1.0155
V_{89}	1.0051
V_{90}	0.9852
V_{91}	0.9807
V_{92}	1.0045
V_{99}	1.0103
V_{100}	1.0171
V_{103}	1.0053
V_{104}	0.9819
V_{105}	0.9757
V_{107}	0.9528
V_{110}	0.9739
V_{111}	0.9805
V_{112}	0.9758
V_{113}	0.9927
V_{116}	1.0056
T_{8-5}	0.9854
T_{26-25}	0.9605
T_{30-17}	0.9601
T_{38-37}	0.9355
T_{63-59}	0.9604
T_{64-61}	0.9849
T_{65-66}	0.9348
T_{68-69}	0.9352
T_{81-82}	0.9358
Q_{c5}	−0.0756
Q_{c34}	0.0083
Q_{c37}	−0.2464
Q_{c44}	0.0016
Q_{c45}	0.0812
Q_{c46}	−0.2410
Q_{c48}	0.0381
Q_{c74}	0.0000
Q_{c79}	0.1230
Q_{c82}	0.0396
Q_{c83}	0.1008
Q_{c105}	0.0000
Q_{c107}	−0.1057
Q_{c110}	0.0375
Power loss (MW)	104.83
Voltage deviation	1.6954
L_{max}	0.0662
CPU time (s)	81.45

Table 7
Optimal value of control variables obtained from SPEA 2 for IEEE 118 bus system.

Variable	
V_{1}	0.9550
V_{4}	0.9981
V_{6}	0.9905
V_{8}	1.0154
V_{10}	1.0479
V_{12}	0.9905
V_{15}	0.9712
V_{18}	0.9734
V_{19}	0.9645
V_{24}	0.9920
V_{25}	1.0500
V_{26}	1.0157
V_{27}	0.9683
V_{31}	0.9678
V_{32}	0.9688
V_{34}	0.9834
V_{36}	0.9803
V_{40}	0.9708
V_{42}	0.9854
V_{46}	1.0058
V_{49}	1.0256
V_{54}	0.9552
V_{55}	0.9561
V_{56}	0.9568
V_{59}	0.9849
V_{61}	0.9953
V_{62}	0.9986
V_{65}	1.0055
V_{66}	1.0500
V_{69}	1.0350
V_{70}	0.9875
V_{72}	0.9807
V_{73}	0.9913
V_{74}	0.9632
V_{76}	0.9430
V_{77}	1.0065
V_{80}	1.0411
V_{85}	0.9866
V_{87}	1.0158
V_{89}	1.0053
V_{90}	0.9852
V_{91}	0.9808
V_{92}	1.0043
V_{99}	1.0106
V_{100}	1.0171
V_{103}	1.0052
V_{104}	0.9817
V_{105}	0.9755
V_{107}	0.9523
V_{110}	0.9736
V_{111}	0.9804
V_{112}	0.9758
V_{113}	0.9926
V_{116}	1.0054
T_{8-5}	0.9852
T_{26-25}	0.9605
T_{30-17}	0.9602
T_{38-37}	0.9352
T_{63-59}	0.9601
T_{64-61}	0.9849
T_{65-66}	0.9348
T_{68-69}	0.9353
T_{81-82}	0.9356
Q_{c5}	-0.1388
Q_{c34}	0.0000
Q_{c37}	−0.1229
Q_{c44}	0.0002
Q_{c45}	0.0858
Q_{c46}	−0.1585
Q_{c48}	0.0013

Table 7 (*continued*)

Variable	
Q_{c74}	0.0000
Q_{c79}	0.1869
Q_{c82}	0.0078
Q_{c83}	0.1136
Q_{c105}	0.0000
Q_{c107}	−0.1121
Q_{c110}	0.0466
Power loss (MW)	101.92
Voltage deviation	1.7332
L_{max}	0.0660
CPU time (s)	98.88

adapted from [31]. The total system active power demand is 42.4200 p.u. and reactive power demand is 14.3800 p.u. at 100 MVA base.

The optimal control variables and active power transmission loss, voltage deviation, L-index and CPU time acquired from the minimization of active power transmission loss, voltage deviation and L-index by using DE have been summed up Tables 3, 4 and 5 respectively. The optimal control variables and active power transmission loss, voltage deviation, L-index and CPU time acquired from the best compromise solution of last iteration from proposed MODE and SPEA 2 have been summed up in Tables 6 and 7 respectively. The convergence characteristics acquired from active power transmission loss, voltage deviation, L-index minimization by using DE have been portrayed in Fig. 7. The distribution of 10 non-dominated solutions acquired from the last iteration of proposed MODE and SPEA 2 for this test system is portrayed in Fig. 8. Fig. 8 portrays the relationship of active power transmission loss, voltage deviation and L-index of nondominated solutions.

Conclusion

This paper studies MORPD problem which is formulated as a multi-objective optimization problem by reckoning minimization of active power transmission loss, minimization of voltage deviation and maximization of voltage stability as competing objectives. Test results acquired from MODE have been compared with those acquired from SPEA 2. The proposed MODE based MORPD problem assists a power system operator to acquire superior dispatch decisions on the basis of pareto-optimal solutions as compared to SPEA 2.

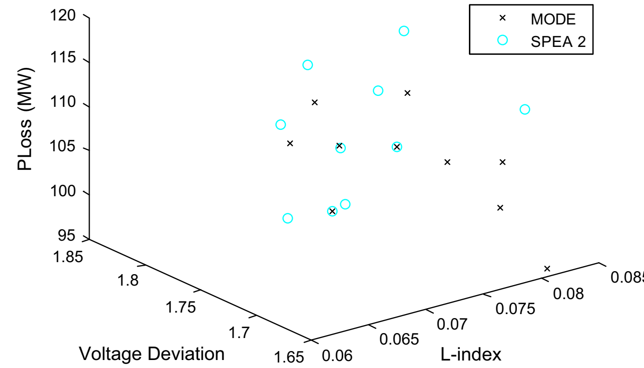

Fig. 8. Pareto-optimal front acquired from the last iteration for IEEE 118 bus system.

References

[1] Dommel H, Tinny W. Optimal power flow solution. IEEE Trans Power Appar Syst 1968;PAS-87(10):1866–76.
[2] Momoh JA, El-Hawary ME, Adapa R. A review of selected optimal power flow literature to 1993 Part I & II. IEEE Trans Power Syst 1999;14(1):96–111.
[3] Lee K, Park Y, Ortiz J. A united approach to optimal real and reactive power dispatch. IEEE Trans Power Appar Syst 1985;PAS-104(5):1147–53.
[4] Quintana VH, Santos-Nieto M. Reactive power-dispatch by successive quadratic programming. IEEE Trans Energy Conver 1989;4(3):425–35.
[5] Granville S. Optimal reactive dispatch through interior point methods. IEEE Trans Power Syst 1994;9(1):136–46.
[6] Wu QH, Ma JT. Power system optimal reactive power dispatch using evolutionary programming. IEEE Trans Power Syst 1995;10(3):1243–9.
[7] Wu QH, Cao YJ, Wen JY. Optimal reactive power dispatch using an adaptive genetic algorithm. Electr Power Energy Syst 1998;20(8):563–9.

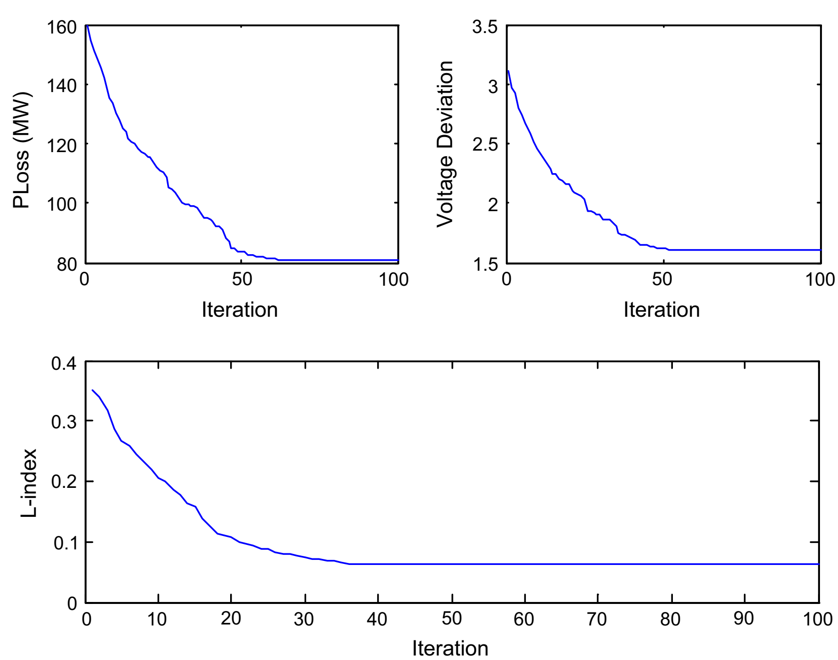

Fig. 7. Active power loss, voltage deviation and L-index convergence characteristics of IEEE 118 bus system.

[8] Yoshida H, Kawata K, Fukuyama Y, Takamura S, Nakanishi Y. A particle swarm optimization for reactive power and voltage control considering voltage security assessment. IEEE Trans Power Syst 2000;15(4):1232–9.
[9] Esmin AAA, Lambert-Torres G, De-Souza ACZ. A hybrid particle swarm optimization applied to loss power minimization. IEEE Trans Power Syst 2005;20(2):859–66.
[10] Tripathy M, Mishra S. Bacterial foraging-based solution to optimize both real power loss and voltage stability limit. IEEE Trans Power Syst 2007;22(1):240–8.
[11] Vlachogiannis JG, Lee KY. Quantum-inspired evolutionary algorithm for real and reactive power dispatch. IEEE Trans Power Syst 2008;23(4):1627–36.
[12] Mahadevan K, Kannan PS. Comprehensive learning particle swarm optimization for reactive power dispatch. Appl Soft Comput 2010;10:641–52.
[13] Khorsandi A, Alimardani A, Vahidi B, Hosseinian SH. Hybrid shuffled frog leaping algorithm and Nelder-Mead simplex search for optimal reactive power dispatch. IET Gen Trans Distrib 2011;5(2):249–56.
[14] Abido MA, Bakhashwain JM. Optimal VAr dispatch using a multiobjective evolutionary algorithm. Electr Power Energy Syst 2005;27(1):13–20.
[15] Hsaio YT, Chaing HD, Liu CC, Chen YL. A computer package for optimal multiobjective VAr planning in large scale power systems. IEEE Trans Power Syst 1994;9(2):668–76.
[16] Chen YL, Ke YL. Multi-objective VAr planning for large-scale power systems using projection-based two-layer simulated annealing algorithms. IEE Proc Gener Transm Distrib 2004;151(4):555–60.
[17] Deb K. Multiobjective optimization using evolutionary algorithms. Chichester (UK): Wiley; 2001.
[18] Sailaja kumari M, Maheswarapu S. Enhanced genetic algorithm based computation technique for multi-objective optimal power flow solution. Int J Electr Power Energy Syst 2010;32(6):736–42.
[19] Jeyadevi S, Baskar S, Babulal CK, Willjuice Iruthayarajan M. Solving multiobjective optimal reactive power dispatch using modified NSGA-II. Int J Electr Power Energy Syst 2011;33:219–28.
[20] Saraswat A, Saini A. Multi-objective optimal reactive power dispatch considering voltage stability in power systems using HFMOEA. Eng Appl Artif Intell 2013;26:390–404.
[21] Ghasemi A, Valipour K, Tohidi A. Multi objective optimal reactive power dispatch using a new multi objective strategy. Electr Pow Energy Syst 2014;57:318–34.
[22] Srinivas N, Deb K. Multi-objective function optimization using nondominated sorting genetic algorithms. Evol Comp 1995;2(3):221–48.
[23] Deb K, Pratap A, Agarwal S, Meyarivan T. A fast and elitist multiobjective genetic algorithm: NSGA-II. IEEE Trans Evol Comput April 2002;6(2):182–97.
[24] Babu BV, Anbarasu B. Multi-objective differential evolution (MODE): an evolutionary algorithm for multi-objective optimization problems (MOOPs). In: Proceedings of the third international conference on computational intelligence, robotics, and autonomous systems (CIRAS-2005), Singapore, December 13–16, 2005.
[25] Zitzler E, Laumanns M, Thiele L. SPEA2: improving the strength pareto evolutionary algorithm. Technical report TIK – report 103, Zurich (Switzerland): Swiss Federal Institute of Technology (ETH); May 2001.
[26] Storn R, Price KV. Differential evolution – a simple and efficient heuristic for global optimization over continuous spaces. J Glob Optim 1997;11(4):341–59.
[27] Price KV, Storn R, Lampinen J. Differential evolution: a practical approach to global optimization. Berlin: Springer-Verlag; 2005.
[28] IEEE Working Group: "Voltage stability of power systems: concepts, analytical tools and industry experience",.IEEE Special Publication 90TH0358-2-PWR; 1990.
[29] Kessel P, Glavitsch H. Estimating the voltage stability of a power system. IEEE Trans Power Deliv 1986;1(3):346–54.
[30] The IEEE 57-bus test system [online], available at <http://www.ee.washington.edu/research/pstca/pf57/pg_tca57bus.htm>.
[31] The IEEE 118-bus test system [online], available at <http://www.ee.washington.edu/research/pstca/pf118/pg_tca118bus.htm>.